Internal Plasma Structure Measurement in a Miniature Microwave Discharge Ion Thruster

IEPC-2007-101

Presented at the 30th International Electric Propulsion Conference, Florence, Italy
September 17-20, 2007

Shinya KONDO*, Takayuki CHIKAOKA†, Teppei TSURU‡, Naoji YAMAMOTO§ and Hideki NAKASHIMA**
Department of Advanced Energy Engineering Science, Kyushu University
6-1 Kasuga-koen, kasuga, Fukuoka 816-8580, JAPAN

Amane MAJIMA††, Takao YAMADA‡‡, Kentaro TOMITA§§ and Kiichiro UCHINO***
Department of Applied Science for Electronics and Materials, Kyushu University
6-1 Kasuga-koen, kasuga, Fukuoka 816-8580, JAPAN

Abstract: Internal plasma structure was investigated in a 30 W class miniature microwave discharge ion thruster in order to understand the mechanism of plasma production and loss. The spatial distribution of the plasma property was measured using a visible ion thruster. This result shows that most ionization is occurring in the magnetic tube. The electron number density and the electron temperature were measured by laser Thomson scattering (LTS). The plasma parameters in the miniature microwave discharge ion thruster were successfully measured by means of LTS for the first time. The results from the LTS are the electron density $n_e = 1.1\times10^{18}$ m^{-3} and the electron temperature $T_e = 2.9$ eV. The measured n_e and T_e values were found to be consistent with the high ion current achieved by this thruster.

Nomenclature

c	=	velocity of light
$d\sigma$	=	differential scattering cross section
e	=	electronic charge
E_L	=	laser energy
F	=	thrust
G	=	observed scattering spectrum

* Graduate student, Department of Advanced Energy Engineering Science, shinya@aees.kyushu-u.ac.jp
† Graduate student, Department of Advanced Energy Engineering Science, chikaoka@aees.kyushu-u.ac.jp
‡ Graduate student, Department of Advanced Energy Engineering Science, tsuru@aees.kyushu-u.ac.jp
§ Research Associate, Department of Advanced Energy Engineering Science, yamamoto@aees.kyushu-u.ac.jp
** Professor, Department of Advanced Energy Engineering Science, nakasima@aees.kyushu-u.ac.jp
†† Graduate student, Department of Applied Science for Electronics and Materials, majimaa6@asem.kyushu-u.ac.jp
‡‡ Graduate student, Department of Applied Science for Electronics and Materials, yamadat6@asem.kyushu-u.ac.jp
§§ Research Associate, Department of Applied Science for Electronics and Materials, tomita@ence.kyushu-u.ac.jp
*** Professor, Department of Applied Science for Electronics and Materials, uchino@asem.kyushu-u.ac.jp

$h \cdot \upsilon$ = photon energy
I_b = ion beam current
I_{sp} = specific impulse
I_T = intensity of Thomson scattering light
I_R = intensity of Rayleigh scattering light
I_0 = intensity of incident laser
$\boldsymbol{k}$ = wave vector
$\boldsymbol{k}_i$, = wave vectors of the incident light,
$\boldsymbol{k}_s$ = vectors of the scattered light
ℓ = scattering length
m_e = electron mass
m_i = ion mass
$\dot{m}$ = mass flow rate for ion source
N_{mag} = number of magnets
n_e = electron density
N_s = Thomson scattered photon number
n_0 = neutral density of Rayleigh scattering
P_i = incident microwave power
r_0 = Classical electron radius
S = laser beam cross section,
$S' \cdot l$ = scattering volume
T_e = electron temperature
V_b = beam voltage
V_B = Bohm velocity
ΔV = scattering volume
α = scattering parameter
ε_c = ion production cost
$\delta\lambda$ = infinite small wave length
$\Delta\Omega$ = solid angle of observation
η = the transmission coefficient
η_t = thrust efficiency
η_u = propellant utilization
θ = angle between wave number vector of incident laser and wave number vector of scattering light
λ = wavelength of incident laser
λ_i = wavelength of incident laser
λ_D = Debye length
$\Delta\lambda$ = difference between scattering wave length and laser wave length
$\Delta\lambda_{1/2}$ = half width at half maximum of Thomson scattering spectrum
ξ = angle between y axis and wave number vector of scattering light vector projected vector on x-z plane
σ_T = Thomson scattering cross section per unit solid angle

I. Introduction

THE demand for mN class miniature propulsion systems is expected to grow in the future[1] for small satellites, since the adoption of small satellites, with their flexibility, short development time and low cost, has been a breakthrough in space applications.[2, 3] Until recently, however, size restrictions have limited the capacity of the available propulsion systems.

Since an ion thruster produces high thrust efficiency with a specific impulse of 3,000-8,000 sec, the adoption of ion thruster into small satellites will expand their ability, that is, missions such as Mars exploration and self-disposal of satellites would become possible. The miniature ion thrusters can also be used for precise high-stability attitude and position control in large spacecrafts, as well as for primary propulsion of microsatellites.[4]

Several studies have been conducted on the miniature ion thruster.[5-7] Wirz et al. showed good performance of a 30 mm Miniature Xenon Ion (MiXI) thruster[5], that is, the propellant utilization and the ion beam production cost were 0.8 and 500 W/A, for 0.2 sccm of mass flow rate. An electron bombardment-type ion source was used for ion production, so that operation time was limited by the thermionic cathode lifetime. A microwave discharge ion source would offer a potentially longer thruster lifetime than the electron bombardment-type, since it would be free from contamination and degradation of electron emission capacity.[8, 9]

The thrust performance of miniature microwave discharge ion thrusters has thus far been inferior to conventional ion thrusters, however, because of the high cost of ion production due to poor microwave-plasma coupling as well as high losses from ion and electron collisions with the walls.[10] This type of ion source has a magnetic tube formed by a magnetic circuit and it also has an antenna to emit microwaves. A magnetic tube works as a virtual cathode, since trapped electrons gain energy from the microwaves by electron cyclotrons resonance (ECR) heating and they ionize neutral atoms.[11] For effective microwave-to-plasma energy transfer, the antenna will contact the ECR layer, since a high electric field appears in the vicinity of the antenna.[12] On the other hand, a magnetic confinement also affects the performance of the ion source. Indeed, the magnetic field configuration of this thruster affects the thrust performance.[13]

The aim of this study is to measure the internal plasma structure of this thruster and to understand the mechanism of plasma production and loss to improve the thrust performance. Internal plasma structure would help understand the mechanism. However, it is difficult to measure inter properties of the plasma, since the ion thruster is so small that we cannot insert a measurement equipment without perturbations. Therefore, two nonintrusive optical methods were used to measure internal plasma structure. At first, plasma emission from discharge chamber was measured to investigate the spatial distribution of plasma property by using a visible ion thruster. Next, plasma property in the discharge chamber were measured by laser Thomson scattering(LTS).

II. Laser Thomson Scattering

LTS is the scattering of laser radiation by free charged particles, when the photon energy is small compared with the energy equivalent of the rest mass of the charged particles. The energy lost by the radiation is accounted for by classical theory as a result of the radiation emitted by the charged particles when they are accelerated in the transverse electric field of the radiation. Because the electron mass is several orders of magnitude less than that of ions, the acceleration of the electron is accordingly larger for a fixed electric field. Therefore, we usually observe LTS only from electrons. The principle and general experimental arrangement of LTS have been described in detail in various references. [14-18] Briefly explanations of the estimation of T_e and N_e is as follows.

The Thomson scattering intensity, $I_T(\Delta\lambda,\theta)$ is described as

$$I_T(\Delta\lambda,\theta)\Delta\Omega\delta\lambda = I_0 n_e \Delta V \mathrm{d}\sigma_T(\Delta\lambda,\theta)\Delta\Omega\delta\lambda \tag{1}$$

The proportionality constants, differential Thomson scattering cross section, $\mathrm{d}\sigma_T(\Delta\lambda,\theta)$ is described as

$$\mathrm{d}\sigma_T(\Delta\lambda,\theta) = r_0^2 \left[1 - \sin^2\theta \cos^2\xi\right] \cdot S(\Delta\lambda,\theta) \tag{2}$$

The scattering parameter is defined by

$$\alpha = \frac{1}{|\boldsymbol{k}|\lambda_D}, \quad |\boldsymbol{k}| = |\boldsymbol{k}_s - \boldsymbol{k}_i| = \frac{4\pi}{\lambda_i}\sin\frac{\theta}{2} \tag{3}$$

When α is well below 1, the scattering is called the "incoherent scattering" and consists of simple addition of contributions from individual electrons in the plasma. For the present experimental condition, the scattering is in this incoherent domain, e.g., α= 0.003 from typical measured values of electron density (N_e = 1 x 10^{18} m^{-3}) and electron temperature (T_e= 3 eV); the wavelength of a YAG laser/SHG (532 nm) and a scattering angle of 90°.

Because motion of the electrons causes the scattered lights to be Doppler-shifted from the laser wavelength, the scattered spectrum reflects the electron velocity distribution. The Doppler-shift, Δλ, is expressed as

$$\Delta\lambda = 2v\sin(\theta/2)\lambda_i / c \tag{4}$$

So, if the electron velocity distribution is assumed as to be Maxwellian, $S(\Delta\lambda,\theta)$ is given as follows

$$S(\Delta\lambda,\theta) = \left(\frac{m_e}{2\pi e T_e}\right)^{1/2}\left(\frac{c}{2\lambda_i\sin(\theta/2)}\right)\exp\left\{-\frac{m_e}{2eT_e}\left(\frac{c\Delta\lambda}{2\lambda_i\sin(\theta/2)}\right)^2\right\} \tag{5}$$

Therefore, half width at half maximum of Thomson scattering spectrum is,

$$\Delta\lambda_{T,1/2} = \frac{2\lambda_i \sin(\theta/2)}{c}\sqrt{\frac{2eT_e \ln 2}{m_e}} \tag{6}$$

, though this is convolved with the measured instrument function of width 0.54 nm, which was the consequence of an entrance slit width of 0.1 mm, and a double-monochromator reciprocal dispersion of 1 nm/mm. So, taking the deconvolution of the instrumental function into account is needed.

Also, the scattered light intensity is proportional to the electron density n_e as shown in Eq.1. If the optics are absolutely calibrated, the scattered light intensity integrated over the spectrum yields an absolute electron density. Such an absolute calibration is usually carried out in situ by the Rayleigh scattering from a gas with known scattering cross section which fills the discharge chamber at a certain density. The intensity of Rayleigh scattering is described as follow,

$$I_R(\Delta\lambda,\theta)\Delta\Omega\delta\lambda = I_0 n_0 \Delta V d\sigma_R(\Delta\lambda,\theta)\Delta\Omega\delta\lambda \tag{7}$$

Hence, the number density of electron is estimated as

$$n_e = n_0 \frac{d\sigma_R(\Delta\lambda,\theta)}{d\sigma_T(\Delta\lambda,\theta)} \frac{I_T(\Delta\lambda,\theta)}{I_R\Delta\lambda,\theta)} = n_0 \frac{d\sigma_R(\Delta\lambda=0,\theta)}{r_0^2[1@\sin^2\theta\cos^2\xi]} \frac{I_T(\Delta\lambda,\theta)}{I_R} \frac{1}{G(\Delta\lambda,\theta)} \tag{8}$$

III. Miniature Microwave Ion Thruster

The cross section of a 30 W class miniature microwave discharge ion thruster is shown in Fig. 1. The inner diameter is 21 mm and the size of the thruster is 50 mm×50 mm×30 mm. The ion source consists of a magnetic circuit, which has several Samarium Cobalt (Sm-Co) permanent magnets and iron yokes. The magnetic flux density in the discharge chamber can be changed by changing the numbers of the permanent magnets. Microwave power at 2.45 GHz was fed through a coaxial line and into an antenna. A DC block with a loss of 0.43 dB at 2.45 GHz was inserted to protect the microwave amplifier, as shown in Fig. 2. The screen grid and ion source were biased to +1,500 V with respect to ground and the acceleration grid was set to -300 V. The extracted ion beam was estimated as the current through the screen power supply minus the current through the accelerator power supply. The validity of this method was shown in our previous study.[10] A neutralizer was not used in this study, as there is little difference between the extracted ion beam current without a neutralizer and that with a filament neutralizer (ϕ = 0.2 mm×100 mm, 2% thoriated tungsten). There are several candidates for the neutralizer of this thruster, including a field emission cathode,[20, 21] a filament cathode, a internal conduction cathode,[22] and a microwave discharge cathode.[23] A miniature microwave discharge neutralizer is under development, although it has thus far shown poor performance,[23] with an electron current of 15 mA for incident microwave power = 4 W and xenon mass flow rate = 0.005 mg/s. A star antenna is used, since it showed good performance in our previous

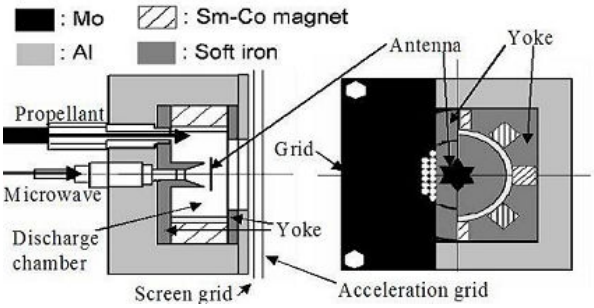

Figure 1. Cross-section of miniature ion thruster developed at Kyushu University

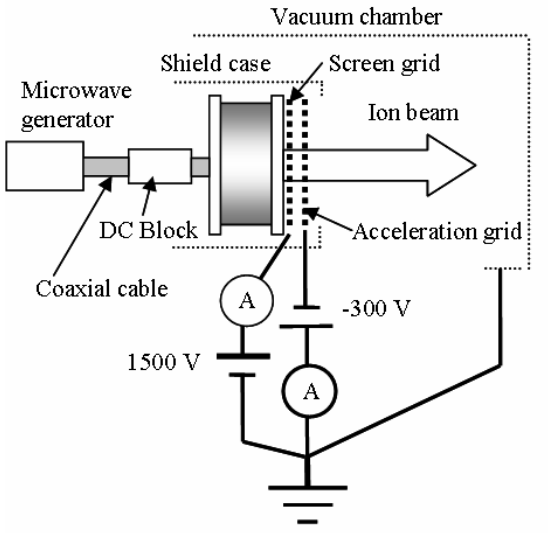

Figure 2. Schematic of electric circuit.

study.[19] The antenna is inscribed in a 9 mm diameter circle and is made of molybdenum. The thickness of it is 1 mm. The antenna lifetime of this thruster may not be a formidable challenge, since the neutralizer adopted in HAYABUSA has an antenna and demonstrated lifetime in excess of 14,000 hrs. In addition, it hardly worn out after one hundred operation, as shown in Fig. 3. The tip of the antenna is inserted into the magnetic tube formed by the magnetic circuit.

Flat circlu grids were used to extract the ion beam. The geometric parameters are shown in Table 1. This geometry was designed using a numerical analysis code developed by Arakawa et al.[24] The grid is made of molybdenum and ceramic cylinders are used as the isolators between the two grids. The gap between the grids is 0.2 mm and the ion beam diameter is 16 mm.

Pure xenon gas (99.999% pure) was used as the propellant. A thermal mass flow controller (full scale = 3 sccm) with a flow accuracy of $\pm 0.7\%$ of rate and $\pm 0.2\%$ F.S. was used. A 0.6 m diameter by 1 m long vacuum chamber was used in the experiments. The pumping system comprised a cryo-pump and a turbo molecular pump. The background pressure was maintained below 1.2×10^{-3} Pa for most of the operating conditions.

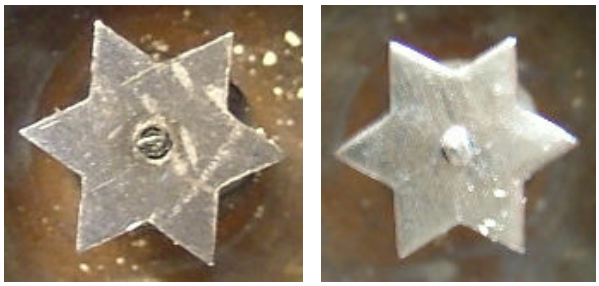

(a) **(b)**

Figure 3. Photo of antennas
(a) before operation (b) after 100 hours operation

Table 1. Grid Parameter

Parameter	Screen	Acceleration
Open area ratio, %	51	16
Hole diameter, mm	1.20	0.70
Potential, V	1500	-300
Thickness, mm	0.30	
Hole pitch, mm	1.20	
Material	molybdenum	
Grid gap, mm	0.20	
Number of holes	91	

Figure 4 shows the relation between incident microwave power and ion beam current for three mass flow rate $\dot{m}$. The ion beam currents are increased with incident microwave power, P_i for a given mass flow rate. And the ion beam currents are increased with mass flow rate, for a given P_i. For P_i=8 W, $\dot{m}$ = 0.018 mg/s and V_b=1,500 V, the ion beam currents is 13.1 mA, while for P_i=16 W, $\dot{m}$ = 0.036 mg/s and V_b=1,500 V, the ion beam currents is 22.5 mA. The ion beam current density in the vicinity of grids for the previous condition is 120 A/m^2, which is about four times larger than that of the NSTAR ion engine.[30] This suggests that plasma density in the discharge chamber would be higher than that of NSTAR. Figure 5 shows the thrust performance for the three flow rates. The propellant utilization decreases with an increase in mass flow rate for a given level of power, since specific energy decreases with an increase in the mass flow rate. The thrust performance of the miniature ion engine, that is, η_u, ε_C, F, I_{sp} and η_t are 0.91, 610 W/A, 0.79 mN, 4.1×10^3 sec and 0.57, respectively at $\dot{m}$ =0.019 mg/s, and P_i = 8 W. For practical applications, some improvement in the performance of the ion engine and drastic improvement of the neutralizer are needed. In addition, lightweight, efficient microwave power supplies are also required for its practical use.

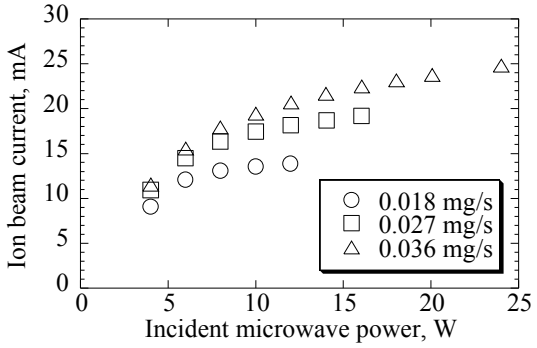

Figure 4. ion beam current for different levels of ion production

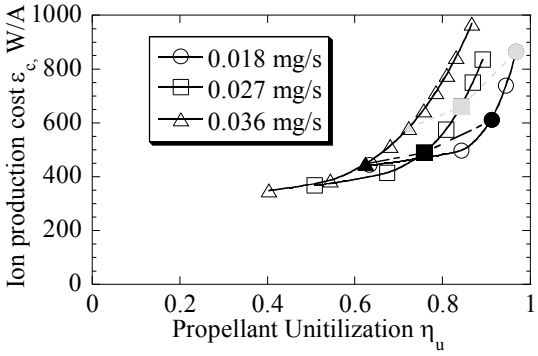

Figure 5. Thrust performance of miniature ion thruster

IV. Experimental Equipment

A. Visible Ion Thruster Measurement

A picture of the visible ion thruster is shown in Fig. 6. In order to see the inside of the discharge chamber, the wall of the discharge chamber is made of BK7glass. The inner diameter is 20.4 mm and the height is 12 mm. Schematic of experimental setup is shown in Fig. 7. Emission from discharge chamber was detected by CCD camera(QImaging,Retiga2000R) through a band-pass filter. The center wavelength of this band-path filter is 488± 0.2 nm and FWMH is 1±0.2 nm. The transition data of this measurement was shown in Table 1 quoted from NIST databese.[25] Xe was used as a propellant gas.

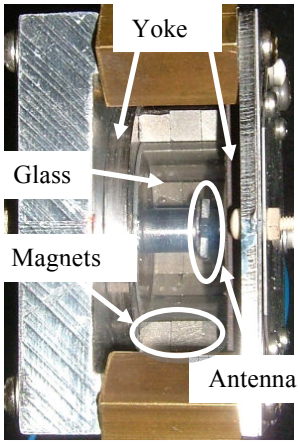

Figure 6. Photo of visible ion thruster

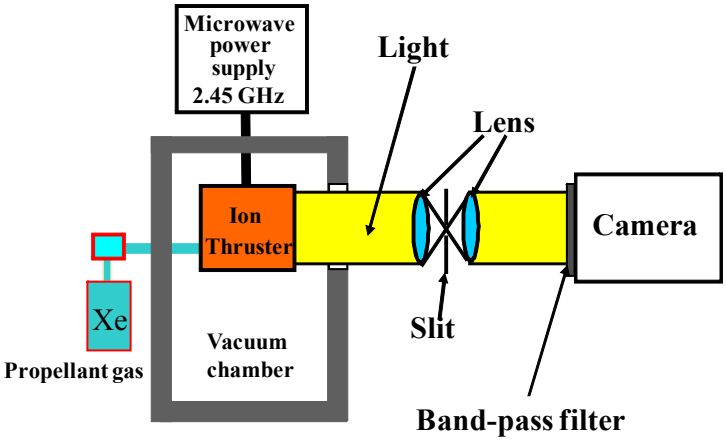

Figure 7. Schematic of spectroscopic measurement system

Table 2 Coefficients of XeII spectrum in the vicinity of 488 nm

	wavelength, nm	A_{ki}, s^{-1}	E_i, eV	E_k, eV	Configurations	g_i	g_k
Xe II	487.650	6.3×10^7	13.584086	- 16.125887	$5p^4(^1D_2)6s$ - $5p^4(^1D_2)6p$	6	- 8

B. Laser Thomson Scattering

Figure 8 shows an experimental setup of LTS measurements on the miniature microwave discharge ion thruster. For the LTS measurements, Kr was used as a working gas, although the thrust performance using xenon as a propellant is superior to that using krypton. Previous experiments to study discharge plasmas containing Xe using LTS[26] concluded the possibility of some laser perturbation effects on the discharge media, when using the second harmonic of the Nd:YAG laser as a light source, while no effect was observed for gas containing Kr. There can be various interpretations of the difference of the effects on discharge media by the laser irradiation, it is due to photo-ionizations of excited Xe atoms[27]; Xe atoms at the ground state (ionization potential 12.1 eV) were ionized by the laser(wavelength 532 nm and photon energy 2.3 eV). Special care should be considered to avoid any laser perturbation effects when applying LTS to study the discharge properties of such gas mixture.

In order to measure the scattering light inside the discharge chamber, two small holes (ϕ= 2 mm) to inject the laser and another hole (ϕ=5 mm) to collect scattering light were made. A ϕ= 5 mm hole was made at the angle of 90 degree from the laser pass.(see Fig. 8)

The light source was the second harmonics beam of a Nd:YAG laser having a wavelength of 532 nm with an energy of 150 mJ, a repetition rate of 10 Hz, a pulse width of 6 ns and a beam divergence of 0.6 mrad. The measurement point is 2 mm downstream of the antenna in the *z* axis, as shown in Fig. 9. The laser beam was focused

at the distance of 2 mm from the tip of the microwave discharge antenna through a focusing lens (f=300 mm). The size of the focal spot was estimated to be 0.08 mm in diameter by observing the spatial profile of Rayleigh scattering from 300 Torr nitrogen gas. Scattered light from the plasma was focused onto the entrance slit of the double monochromator with two achromatic lens of f = 350 mm and f = 250 mm. The scattering volume was 0.08×0.1×1 mm^3, determined by the laser beam size, the slit width and the slit height, respectively. The solid angle of observation was about 0.025 sr. The scattered light was dispersed by passing through the double monochromator, and was detected by a photomultiplier tube (Hamamatsu, R943-02, quantum efficiency ~10%).

The development of LTS started by using a single-pulse ruby laser for high-temperature plasma studies, and resulted in the confirmation of performance claimed for the T-3 tokamak in 1968.[15] In the late '80s. when the demand for electron properties in glow discharge plasmas for material processing grew. Because the electron densities in these plasmas are below 10^{18} m^{-3}, data accumulation is of essence. The Thomson scattered photon number, N_s, is described as

$$N_s = \frac{E_L/S}{h\nu} n_e S' \ell \sigma_T \Delta\Omega \eta, \tag{9}$$

By inserting appropriate numbers for a typical experimental situation (E_L=100 mJ, $h\nu$=4×10^{-19} J for λ=532 nm, S'=S, ℓ =0.001 m, σ_T=9×10^{-30} m^2/sr, $\Delta\Omega$=10^{-3} sr, and η=0.1, we obtain

$$N_s = 2\times10^{-19} N_e. \tag{10}$$

This means that, if the electron density of the plasma is 10^{18} m^{-3}, the Thomson scattered photon number detected for one laser shot is about 0.02. The estimated Thomson scattered photon number is so small that we used photon counting method. The detected Thomson scattered signals were analyzed by a photon counter (Stanford Research Systems Inc., SR430) after accumulating over 5000 laser shots. A data accumulation process technique, taking advantage of the DC or repetitive operation of some discharges, was first suggested for lowering the limiting electron densities by Sakoda et al.[28] Such studies have been performed for ECR, ICP and NLD and, combined with photon counting, have recently achieved a minimum detectable electron density of 5×10^{15} m^{-3}.[29]

Because the probing laser was focused on 2 mm above the tip of antenna, and the discharge chamber was small, many stray lights were generated from the surface of the components, and LTS signals were overwhelmed by them. In order to improve this situation, all components were painted in black and a double-mochromator (f = 575 mm) was used to reduce the stray lights. The double-monochromator used in this experiment could reduce stray light around 10^{-7} at the wavelength of 2 nm from the probing laser, where the LTS signal was observed. After these efforts, we could eliminate strong stray light and detect LTS signals successfully.

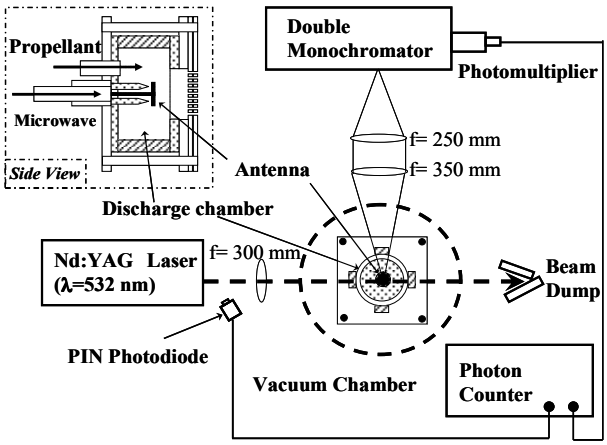

Figure 8. Schematic of LTS system for miniature ion thruster

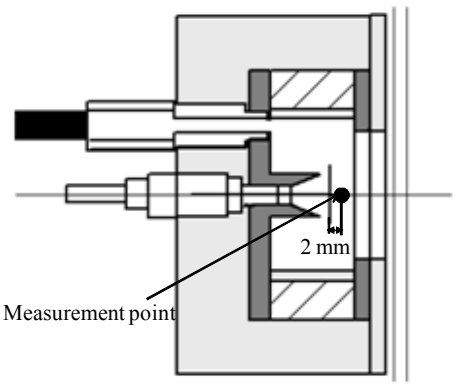

Figure 9. Measurement point of LTS

V. Results and Discussion

A. Visible Ion Thruster Measurement

At first, the influence of wall material on the thrust performance in this ion thruster was investigated. Figure 10 shows the ion beam current for the two wall material, aluminum and glass at mass flow rate = 0.027 mg/s and V_b=1,000 V. As shown in Fig. 10, the ion beam current in each discharge chamber is almost the same. Consequently, it seems that the influence of wall material on the plasma generation is small.

The emission intensity from the discharge chamber is shown in Fig. 11. The intense emission is observed in the magnetic tube. This intensity is integrated along camera direction. Therefore, to get the radial emission profiles, the obtained profiles have to be transformed by the Abel inversion. Assuming the axisymmetry profile, emission intensity profiles are fitted by 16th orders even polynomial function and convert these profiles to a radial emission intensity via the inverse Abel transform. According to our rough estimation, the integrated absorption coefficient of Xe II 487.65 nm is 8 m^{-1}, and then it would be possible to assume this plasma as optically thin plasma.

The emission intensity map at P_i= 8 W and $\dot{m}$ =0.027 mg/s is shown in Fig. 12. There is little emission in the center of the discharge chamber and the most intense emission can be observed in the magnetic tube, which is formed between two yoke. This result shows that most ionization is occurring in the magnetic tube.

Some improvement in Abel inversion is needed to get a more distinct emission distribution map.

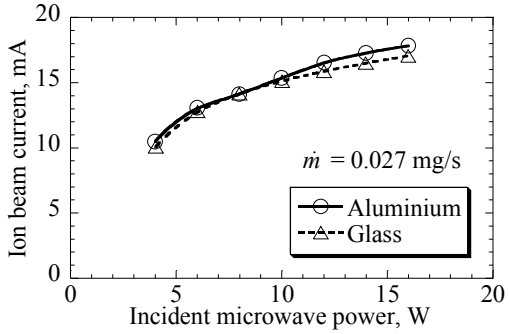

Figure 10. Ion beam current for aluminum and glass discharge camber

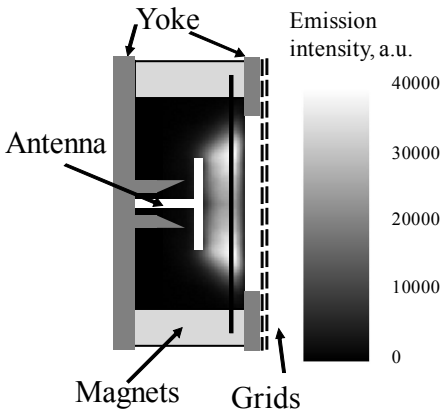

Figure 11. Photo of emission in the discharge camber

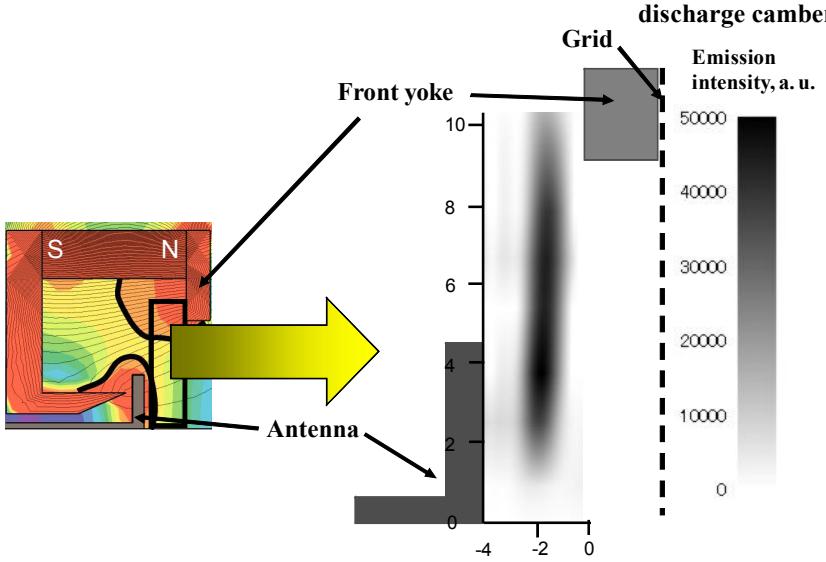

Figure 12. Emission intensity distribution of miniature ion thruster

B. Laser Thomson Scattering

In order to confirm this in terms of the electron density and the velocity distribution, we performed measurements at incident laser energy of 150 mJ, and observed signals from various wavelengths for for $\dot{m}$ = 0.16 mg/s and P_i= 8 W without ion beam extraction. In Fig.13, Thomson scattering intensities are plotted in a logarithmic scale in the ordinate against $(\Delta\lambda)^2$, the square of the differential wavelength from the laser wavelength, the latter being proportional to the electron energy. The solid lines represent Maxwellian distributions at the temperature of 2.9 eV. From the straight line of the Thomson spectrum, we conclude that the electron energy distribution function was Maxwellian. From this spectrum and the Rayleigh scattering calibration using nitrogen gas, n_e and T_e are evaluate to be $(1.1\pm0.2)\times10^{18}$ m^{-3} and 2.9±0.5 eV, respectively.

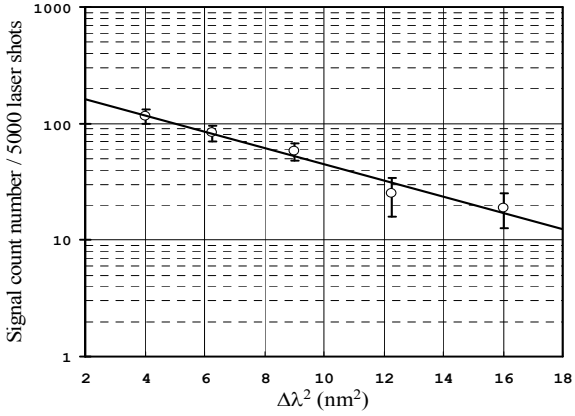

Figure 13. Thomson scattering spectrum.

Next, in order to confirm that the observed signal is truly LTS signal from the discharge chamber plasma, the relation between the incident microwave power and the LTS signal was investigated. Figure 14 shows the LTS signals for various incident laser power from 30 mJ to 150 mJ at $(\Delta\lambda)^2$= 4 nm^2. The LTS signals is linearly increased with incident microwave energy, as shown in this figure. Hence, we conclude that this signal is LTS signal. In addition, the laser irradiation did not influence the measurements for this condition, since fitting error is less than that derived from the experiment.

Here, we discuss the validity of this measurement. According to the Bohm sheath criterion, an ion velocity from the plasma into an ion sheath on a grid is assumed as the Bohm velocity expressed as follows.

$$V_B = \sqrt{\frac{kT_e}{m_i}} \tag{11}$$

Therefore, ion beam current is evaluated as below.

$$I_b = en_e \exp\left(-\frac{1}{2}\right) S\sqrt{\frac{kT_e}{m_i}} \tag{12}$$

Here, e is an electronic charge, k is the Boltzmann constant, m_i is the ion mass and S is the total ion beam extracting area. Under the condition of the LTS measurement, $m_i = 1.4\times10^{-25}$ kg, T_e =2.9 eV, n_e=1.1×10^{18} and $S = 1.0\times10^{-4}$ m^2. Substituting these values, we obtain I_b = 20 mA. On the other hand, from Fig. 15, the ion beam current, which were measured under the condition of the LTS measurement, is evaluated to be 25 mA. Therefore, the values of two ion beam currents evaluated by two different experiments are almost same, considering measurement errors. Therefore, the validity of this measurement is verified.

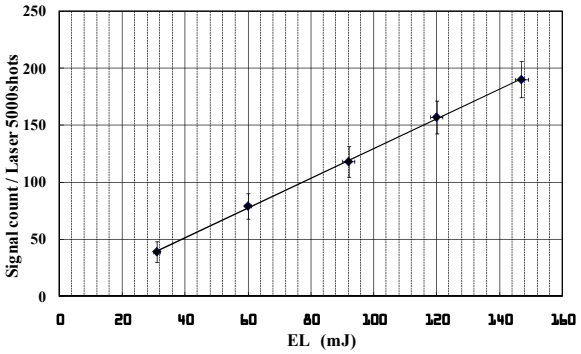

Figure 14. Thomson scattering signal vs incident laser power

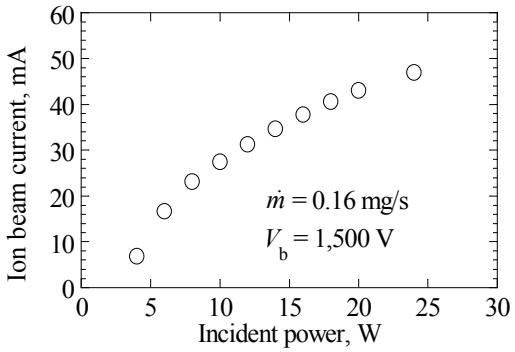

Figure 15. Ion beam current for Kr $\dot{m}$ = 0.16 mg/s and V_b = 1,500 V

From the LTS measurement result, it was confirmed that the electron density in this thruster is several times higher than that of conventional ion engine.[31] This dense electron density leads the high ion beam current density of this engine. In conclusion, plasma parameters in the miniature microwave discharge ion thruster were successfully measured by means of LTS for the first time, and we could confirm that the measured n_e and T_e were found to be consistent with the high ion current achieved by this thruster

VI. Conclusion

The Internal plasma structure of the miniature microwave discharge ion thruster was measured for understanding the mechanism of plasma production and loss to improve the thrust performance.

Using the visible ion thruster, the emission distribution from the Xe II transition at 488 nm was measured. The intense emission can be observed in the magnetic tube. This shows that most ionization is occurring in the magnetic tube. With other various transition lines of Xe II and CR model, it would be possible to estimate the detail electron excitation temperature distribution and relative plasma density distribution.

The plasma parameters in the miniature microwave discharge ion thruster were successfully measured without perturbation by nonintrusive optical methods of LTS for the first time. At P_i = 8 W, and krypton mass flow rate = 0.16 mg/s , n_e and T_e are evaluate to be $(1.1\pm0.2)\times10^{18}$ m^{-3} and 2.9±0.5 eV, respectively. We could confirm that the measured n_e and T_e were found to be consistent with the high ion current achieved by this thruster.

The adoption of these methods would unveil the plasma production- loss mechanism in the microwave discharge ion thruster and other electric propulsions.

Acknowledgments

The present work was supported by a Grant-in-Aid for Scientific Research (C) (2), No. 16560691, and a Grant-in-Aid for Young Scientists (B), No. 17760638, sponsored by the Japan Society for the Promotion of Science, Japan.

References

[1]Mueller, J., "Thruster Options for Microspacecraft: A Review and Evaluation of State-of-the Art and Emerging Technologies," Micropropulsion for Small Spacecraft, edited by Micci, M. M., and Ketsdever, A.. D., Progress in Astronautics and Aeronautics, AIAA, Reston, VA, 2000, pp. 45–137.

[2]Kato, M., Takayama, S., Nakamura, U., Yoshihara, k., and Hashimoto, H., "Road Map of Small Satellite in JAXA," 56th International Astronautics Congress Paper, IAC-05.B5.6.B.01, Fukuoka, Oct., 2005

[3]Sahara H., Nakasuka, S., and Kobayashi, C., "Propulsion System for Panel Extension Satellite (PETSAT)," AIAA Paper 2005-3956, July 2005.

[4]Kilter, M., "Micropropulsion Technology Assessment for DAWIN," Masters Thesis, Luleå University of Technology, 2004.

[5]Wirz, R. E., "Discharge Plasma Processes of Ring-Cusp Ion thrusters," Ph D. Diss., California Institute of Technology, 2005.

[6]Mistoco, V., Bilén, S., and Micci, M., "Development and Chamber Testing of a Miniature Radio-frequency Ion Thruster for Microspacecraft," AIAA paper 2004-4124, July 2004.

[7]Yoshinori Nakayama, Ikkoh Funaki, Hitoshi Kuninaka and Hideki Nakashima, "Experimental Evaluation of Miniaturized Ion Thruster with Microwave Discharge," Journal of the Japan Society for Aeronautical and Space Sciences, 53 (621),2005, pp.461-466 (in Japanese)

[8]Kuninaka, H. and Satori, S., "Development and Demonstration of Cathodeless Electron Cyclotron Resonance Ion Thruster," Journal of Propulsion and Power, Vol. 14, No. 6, 1998, pp.1022-1026.

[9]Funaki, I., Kuninaka, H, Toki, K., Shimizu, Y., Nishiyama, K., and Horiuchi Y., "Verification Tests of Carbon-Carbon Composite Grids for Microwave Discharge Ion Thruster," Journal of Propulsion and Power, Vol. 18 No. 1, 2002, pp. 169-175.

[10]Takao, Y., Miyamoto, T., Kataharada, H., Nakashima, H., Masui, H., Kai, T., Ijiri, H., Mori, and Y., Yamamoto, N., "Development of Small-Scale Ion Thruster Utilizing Microwave Discharge Plasma," Proceedings of the 24th International Symposium on Space Technology and Science, ed. by J. Onodera, Japan Society for Aeronautical and Space Sciences and Organizing Committee of the 24th ISTS, Tokyo, Japan, 2004, pp. 161-166.

[11]Funaki, I., Kuninaka, H., Toki, K., "Plasma Characterization of a 10-cm Diameter Microwave Discharge Ion Thruster," Journal of Propulsion and Power, Vol. 20, No. 4, 2004, pp. 718-726.

[12]Masui, H., Tashiro, Y., Yamamoto, N., Nakashima, H. and Funaki, I., "Analysis of the electron and microwave behavior in microwave discharge neutralizer," Transactions of The Japan Society for Aeronautical and Space Sciences, (to be published)

[13]Chikaoka, T., Kondo, S., et.al., "Magnetic Field Configuration Effects on Thrust Performance of Miniature Microwave Discharge Ion Engine," PROCEEDINGS OF THE TWENTY-FIFTH INTERNATIONAL SYMPOSIUMU ON SPACE TECHNOLOGY, Japan Society for Aeronautical and Space Sciences and Organizing Committee of the 25th ISTS, 2006, pp.254-259.

[14]Kunze, H. J., "*The laser as a tool for plasma diagnostic*," in *Plasma diagnostics*, W. Lochte-Holtgreven, Ed. Amestrdam: Noth- Holland Publishing Company, 1968. pp.550.

[15]Evans, D. E., and Katzenstein, J., "Laser light scattering in laboratory plasmas," Rep. Prog. Phys., vol. 32, pp.207–271, 1969.

[16]DeSelva, A. W. and Goldenbaum, G. C., "Plasma diagnostics by light scattering," in *Methods of Experimental Physics*, vol. 9-Plasma Physics, part A, H. R. Griem and R. H. Lovberg, Ed. New York: Academic Press, 1970. pp.61-113

[17]Sheffield. J., *Plasma Scattering of Electromagnetic Radiation*. New York: Academic Press, 1975.

[18]Muraoka, K., Uchino, K., and Bowden, M. D., "Diagnostics of low-density glow discharge plasmas using Thomson scattering," Plasma Phys. Control. Fusion, vol. 40, pp.1221–1239, July 1998.

[19]Yamamoto, N., Masui, H., Kataharada, H., Nakashima, H., and Takao, Y., "Antenna Configuration Effects on Thrust Performance of Miniature Microwave Discharge Ion Engine," Journal of Propulsion and Power Technical Note, (to be published)

[20]Okawa, Y., Kitamura, S., Kawamoto, S., Iseki, Y., Hashimoto, K., and Noda, E., "An Experimental Study On Carbon Nanotube Cathodes For Electrodynamic Tether Propulsion," 56th International Astronautics Congress Paper, IAC-05-C4.4.07, Oct. 2005.

[21]Yamamoto, A., Nakai, H., Kaneko, N., Nakashizu, T., Ohsawa, S., Sugimura, T., and Ikeda, M., "The Research On the Carbon Nano Tube Cathode," Proceedings of the 2003 Particle Accelerator Conference, pp.3326-3328, 2003.

[22]Wirz, R., Gale, M., Mueller, J., and Marrese, C., "Miniature Ion Thrusters for Precision Formation Flying," AIAA paper 2004-4115, July 2004.

[23]Tanisho, M., Kataharada, H., Yamamoto, N., Nakashima, H., "A Miniaturized Ion Thruster and Neutralizer with Microwave Discharge," 56th International Astronautics Congress Paper, IAC-05-CIAC-05-C4.4.02, 2005.

[24]Nakano, M. , Tachibana, T., and Arakawa, Y. , "A Scaling Law of the Life Estimation of the Three-Grid Optics for an Ion Engin," Transactions of the Japan Society for Aeronautical and Space Sciences, Vol.45, No.149, 2002, pp.154-161.

[25] NIST Atomic Spectra Database, http://physics.nist.gov/cgi-bin/AtData/main_asd

[26]Uchino, K., Kubo, Y., Muraoka, K., sakoda, T., Yamakoshi, h., Kato, M., Takahashi, A., and Maeda, M., "Investigation of electron density and velocity distribution in high pressure discharges for excimer laser pumping using laser Thomson scattering," J. Appl. Phys., vol. 70, pp.41–45, July 1991

[27]Kim, Y. K., Tomita, K., Hassaballa, S., Uchino, K., Muraoka, K., Hatanaka, H., Kim, Y. M., Lee, S. E., Son, S. H. and Jang, S. H., "Development of an Infrared Laser Thomson Scattering System for Measurements of Electron Density and Electron Temperature of a PDP Micro-discharge Plasma," SID INTERNATIONAL SYMPOSIUM DIGEST OF TECHNICAL PAPERS 2004, VOL 35; BOOK 1, pages 550-553

[28]Sakoda, T., Momii, S. Uchino K., Muraoka, K., Bowden, M., Maeda, M., Manabe, Y., Kitagawa, M., and Kimura, T., "Thomson Scattering diagnostics of an ECR Processing Plasma," Jpn. J. Appl. Phys., vol. 30, pp.L1425–L1427, August 1991.

[29]Mansour, H. Koyama, M. D. Bowden, K. Uchino, and K Muraoka, "A Laser Thomson scattering System for Low Density Glow Discharge Plasmas," Jpn. J. Appl. Phys., vol. 40, pp.1465–1466, March 2001.

[30]Sovey „J. S., Rawlin, V. K., Patterson, M. J. "Ion Propulsion Development Projects in U.S.: Space Electric Rocket Test I to Deep Space 1" Journal of Propulsion and Power 2001 vol.17 no.3 pp.517-526.

[31]Herman, D., A., and Gallimore, A.,D., "Interrogation of Discharge Chamber Plasma Structure of an Ion Engine Using a High-Speed Probe Positioning System," AIAA paper-2003-5162(2005).